

Migration of Seismic Data

Ernesto Bonomi¹ and Gabriella Cabitza¹

Received October 15, 1993; final March 28, 1994

Prospecting for oil and gas resources poses the problem of determining the geological structure of the earth's crust from indirect measurements. Seismic migration is an acoustic image reconstruction technique based on the inversion of the scalar wave equation. Extensive computation is necessary before reliable information can be extracted from large sets of recorded data. In this paper a collection of "industrial" migration techniques, each giving rise to a data parallel algorithm, is outlined. Computer simulations on synthetic seismic data illustrate the problem and the approach.

KEY WORDS: Seismology; migration; scalar wave equation; parallel computing.

1. INTRODUCTION

The objective of most echo techniques is to reconstruct, without destructive penetration, the geological map of the earth's crust. To first order, the crust is a layered medium composed of unconsolidated formations (sand), consolidated and permeable formations (sandstone), and hard, tight formations (rock), each one with specific continuum mechanical properties (sound velocity, density, etc.). The geological methods of prospecting for oil and gas resources are based on observations of elastic wave fields, treated to a first approximation as acoustic waves.⁽¹⁾ Emitted pressure impulses penetrate the crust and then are backscattered to the surface, where they are detected by an array of receivers, usually one-dimensional. Each receiver, a seismograph or a geophone, produces a trace composed typically of 1500 time intervals of 4 msec each. The time behavior of a single trace depends in a complex way on the inhomogeneities of the earth's crust. Gathered traces, in real cases as many as 2000, represent a local estimate of the compressional wave field. The computation necessary

¹ Parallel Computing, Centre for Advanced Studies, Research and Development in Sardinia, I-09123 Cagliari, Italy.

to extract useful geological information from large sets of data (100 km² areal coverage, up to 100,000 tapes for a field experiment) is extensive.

To reconstruct an acoustic image of the subsurface, the earth is modeled as a complicated distorting lens made of small diffracting points, each with a specific scattering strength. Variations of a ray path through the earth are due to inhomogeneities in the medium. Smooth changes associated with compaction cause rays to be slowly turned or refracted. Fractures and discontinuities between lithological layers, mostly in the vertical direction, cause reflections and diffraction. In the absence of sudden changes in the medium, the only signal detected by the receivers is that of the source shock traveling along the surface.

In the migration process,⁽²⁾ recorded pressure waves are used as initial conditions for a wave field governed by the scalar wave equation, which propagates downward and in reverse time. Two computation phases are necessary to migrate the recorded data: inverse wave field extrapolation and imaging. Using the wave equation, initial data must be transformed into simulated recordings of the pressure field on each virtual plane below the earth's surface. In the imaging phase, scatterer positions, characterized by strong reflection coefficients, can be retrieved from the extrapolated wave field.

To reduce the complexity of the initial data inversion, spatial density variations are ignored. The compressional velocity field, a piecewise function taking values from 0.4 km/sec (sand) up to 7.0 km/sec (granites) which generally increases with depth, is assumed known. The entire migration process is thus based on the *a priori* estimation of the velocity field from well logs or velocity analysis. In complicated geological situations, the velocity model is not accurately known, and it is only by interpreting migrated data that the velocity model is verified. One way to address this paradox is to formulate seismic inversion as an optimization problem; the solution is that velocity field whose seismic response, governed by the wave equation, gives the best fit to surface measurements and thus most accurately locates reflecting surfaces.^(3,4) Elegant numerical simulations have confirmed the validity of this approach on synthetic and on real data,^(5,6) nevertheless its computational cost is today out of reach of most real applications. For this reason, in the oil industry a pragmatic approach is preferred.

Here we present the exploding reflector model and the resulting zero-offset data migration in homogeneous and inhomogeneous media, embedding the most common post-stack migration models in the context of parallel computing. Three downward extrapolation techniques are outlined and illustrated with simulations on synthetic seismic sections. We take advantage of intrinsic concurrency to achieve an efficient data parallel

implementation for each simulation. The description of the conventional method of velocity analysis goes beyond the scope of this article; nevertheless it constitutes a basic step before our inverse process of retrieving the structure of the earth's crust can begin.^(7,8)

2. THEORETICAL FRAMEWORK

In this article the earth's crust is modeled as a two-dimensional half-space: the x axis is horizontal and the z axis is vertical, pointing downward. The methodology can be extended to three spatial dimensions.

Pressure waves are assumed to be traveling at point (x, z) with velocity $c(x, z)$. In homogeneous media, $c(x, z) = c_0$, there is no reflection and waves are fully transmitted; in homogeneous media with spatial variations in c , waves are partially reflected. Any point (x, z) underneath the earth's surface is characterized by a reflection coefficient R , whose angular dependence will be ignored. In the special case where c takes only two values, c_1 and c_2 , with $c_1 \gg c_2$, waves traveling at velocity c_1 are essentially reflected by the discontinuity.

Figure 1 illustrates a simulated seismic experiment: $c(x, z) > 0$ is constant, except on the three segments denoted by R_1 , R_2 , and R_3 , where $c = 0$ (Fig. 1a). An impulsive source is initiated; Figs. 1b–1e show the evolution of the pressure wave: segments R_1 , R_2 , and R_3 act as reflectors. Figure 1f is the corresponding "seismic section," that is, the pressure wave recorded by a horizontal array of receivers containing the source. The straight lines represent the signal propagating along the receiver array, and the hyperbolas represent the signal backscattered by the reflectors.

Let $P(x_s, z_s, x_0, z_0, t)$ denote the pressure measured at time t by a receiver at position (x_0, z_0) after an impulsive source at position (x_s, z_s) has been initiated at $t = 0$. For a given source, the pressure field measured on each (x_0, z_0) , is a solution of

$$\frac{\partial^2 P}{\partial x_0^2} + \frac{\partial^2 P}{\partial z_0^2} - \frac{1}{c(x_0, z_0)^2} \frac{\partial^2 P}{\partial t^2} = 0 \quad (1)$$

Figure 1 is obtained solving Eq. (1), using a multistep time integration scheme and a spectral approximation for spatial derivatives.

For a given receiver, as a consequence of the principle of reciprocity⁽⁹⁾ (transposing source and receiver, the observed wavefield must be unchanged), the pressure field induced by moving the source on each point (x_s, z_s) is also a solution of the scalar wave equation

$$\frac{\partial^2 P}{\partial x_s^2} + \frac{\partial^2 P}{\partial z_s^2} - \frac{1}{c(x_s, z_s)^2} \frac{\partial^2 P}{\partial t^2} = 0 \quad (2)$$

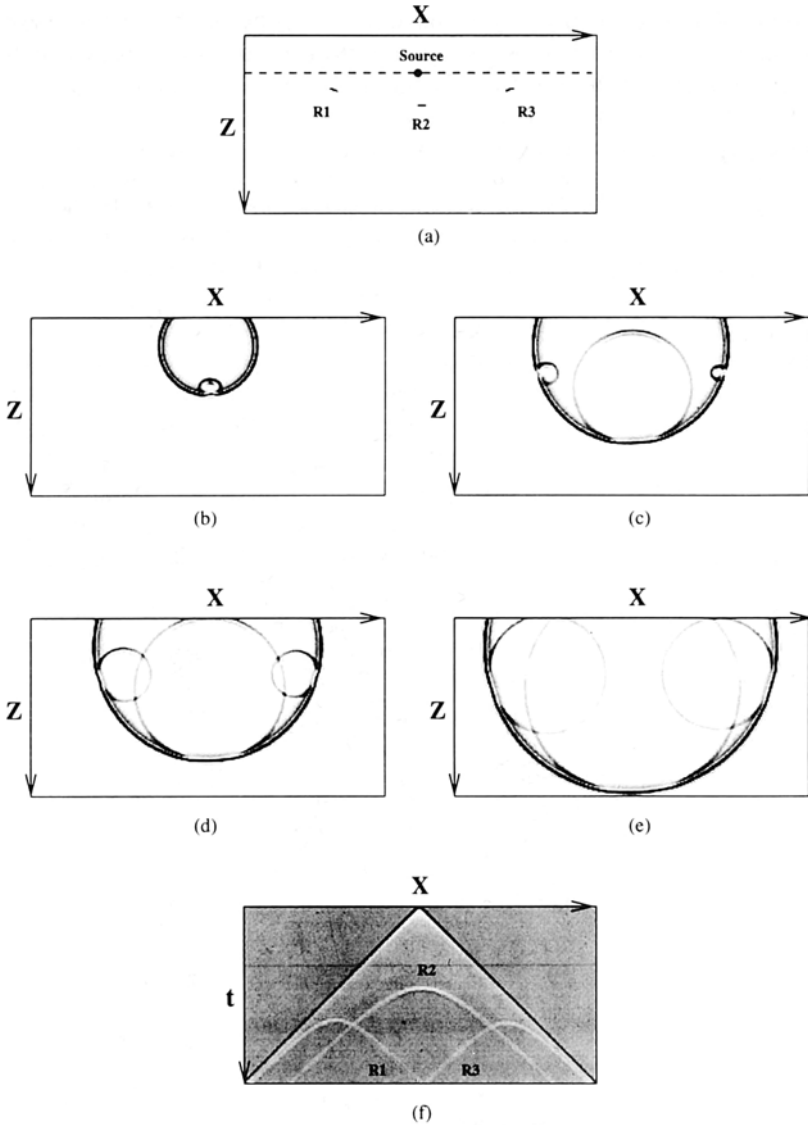


Fig. 1. Simulated seismic experiment (a) Impulsive source, receivers, and velocity model: $c = 1$ km/sec, except on R_1 , R_2 , and R_3 , where $c = 0$ km/sec; (b-e) pressure wave propagation, R_1 , and R_2 , and R_3 act as reflectors; (f) pressure field recorded by the array of receivers; straight lines represent the signal propagating along the array, hyperbolas represent the signal backscattered by the reflectors; $N_x = 256$, $N_z = N_t = 128$, $\Delta X = \Delta Z = 50$ m, $\Delta t = 50$ msec.

Migration⁽¹⁰⁾ is an inversion process which reconstructs the map $R(x, z)$ of local reflectivity from the only available information, the “seismic section” $P(x_s, 0, x_0, 0, t)$ and the velocity field $c(x, z)$. The earth is considered flat and the density field is considered constant throughout the medium.

Introducing appropriate boundary conditions and solving Eqs. (1) and (2) for $P(x_s, z_s, x_0, z_0, t)$, the raw or “pre-stacked” seismic section can be migrated, advancing along the z axis, yielding for each virtual source–receiver pair the value of the pressure as a function of the travel time t . Notice that moving source and receiver downward along ray paths (Fig. 2), reflectors along points of discontinuity in the medium are eventually located at $(x, z) = (x_s, z_s) = (x_0, z_0)$. On these points, R and P are related as follows:

$$R(x, z) \sim P(x, z, x, z, 0) \tag{3}$$

As source and receiver approach each other, the travel time between them goes to zero. $P(x, z, x, z, 0)$ is called the “migrated section.”

Migration of pre-stacked seismic data has the potential to provide a reliable acoustic imaging of the earth. Nevertheless, in the context of a real application, the resulting numerical process is a heavy computational task

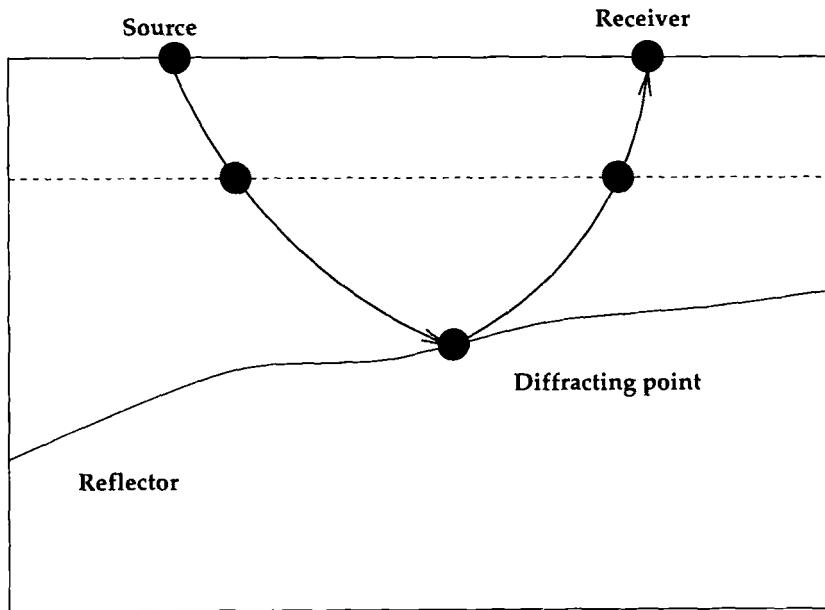


Fig. 2. The earth cross section: during the migration process, source and receiver are collapsed backward along the ray path.

a consequence, an equivalent trace will result from a source initiated at the reflector with the appropriate strength, provided the velocity of the medium is divided by two. This is the so-called "exploding reflector" model. Hence, using the recorded zero-offset wavefield $P(X, 0, t)$ and solving Eq. (9) in reverse time, at time $t=0$ we should obtain an acoustic picture $P(X, Z, 0)$ of the reflectors.

The zero-offset data representation thus implies the powerful analogy between sources and reflectors. But seismic experiments involve kilometers of offset between each source and its receivers. In practice, a pre-processing technique, called stacking, has been developed to approximate zero-offset sections. For a given velocity model, nonzero-offset traces $P(x_s, z_s, x_0, z_0, z_0, t)$, sharing the same midpoint X , are first transformed by hyperbolic coordinate transformations, the "Normal Move-Out" or the "Dip Move-Out" correction, leading to a time-variable shift.⁽¹²⁾ Second, they are averaged, or "stacked" around the midpoint to get a plausible approximation to a zero-offset trace $P(X, 0, t)$. It is worthwhile mentioning that finding the "best" velocity model is then a matter of optimizing a "stack power" function.⁽¹³⁾ So, a stacked seismic section does not correspond to the observations of a real experiment and the consequent migrated section is not an observable wave field.

For many applications, stacked seismic sections are considered as the result of plane-wave experiments. This assumption works well provided reflector locations are of more interest than signal amplitudes. The breakdown of the plane-wave model is the impossibility to incorporate multiple reflections which are present in real seismic traces. Nevertheless, even with this oversimplification, useful results can be obtained.

4. DOWNWARD WAVE EXTRAPOLATION

Let us write in an unusual form the scalar equation (9) for the zero-offset pressure field $P(X, Z, t)$:

$$\frac{\partial^2 P}{\partial Z^2} = \frac{1}{v(X, Z)^2} \frac{\partial^2 P}{\partial t^2} - \frac{\partial^2 P}{\partial X^2} \quad (10)$$

Notice that v is the halved wave velocity, X is the horizontal midpoint variable, and t is the two-way traveling time. Z , the depth, is the advancing variable along which the seismic section $P(X, 0, t)$ must be extrapolated downward. The target is to evaluate the migrated section $P(X, Z, 0)$.

To solve Eq. (10), missing boundary conditions must be restored. For this purpose, we have imposed periodicity of the solution along the X and

t axes. Although this choice may be artificial, it allows us to take advantage of Fourier theory and construct the solution step by step along the Z axis.

4.1. Migration by Phase Shift

Assume that v , the halved wave velocity, is constant. Let $P(X, Z, t)$ be represented by a double Fourier series:

$$P(X, Z, t) = \sum_{k_x} \sum_{\omega} P(k_x, Z, \omega) \exp[i(k_x X + \omega t)] \quad (11)$$

where k_x and ω are respectively the midpoint and the time wave number. By substitution of the Fourier series in Eq. (10), one obtains for each coefficient of Eq. (11) the following second-order ordinary differential equation:

$$\frac{d^2 P(k_x, Z, \omega)}{dZ^2} = -\left(\frac{\omega}{v}\right)^2 \left[1 - \left(\frac{vk_x}{\omega}\right)^2\right] P(k_x, Z, \omega)$$

This equation has one general solution of the form

$$P(k_x, Z, \omega) = A \exp(ik_z Z) + B \exp(-ik_z Z)$$

in which

$$k_z = \frac{\omega}{v} \left[1 - \left(\frac{vk_x}{\omega}\right)^2\right]^{1/2} \quad (12)$$

Equation (12) is the well-known dispersion relation (Fig. 6). A and B , the constants of integration, are independent of Z . The vertical wave number k_z embodies the downward characteristic solution, ($-k_z$) the upward one. Since we are interested in the inverse extrapolation of the seismic section, B must be set to zero and consequently

$$P(k_x, Z, \omega) = P(k_x, 0, \omega) \exp(ik_z Z) \quad (13)$$

where $P(k_x, 0, \omega)$ is the transformed seismic section in the (k_x, ω) domain. Notice that setting B to zero in the general solution, the first derivative of the seismic section along the Z axis is implicitly and unequivocally defined. Substituting Eq. (13) into (11), we get the solution of the inverse problem for constant velocity,

$$P(X, Z, 0) = \sum_{k_x} \sum_{\omega} P(k_x, 0, \omega) \exp[i(k_z Z + k_x X)] \quad (14)$$

Notice that because we are only interested in propagating waves, k_x and ω must be restricted in the summations to those values leading to real values k_z , thus avoiding spurious waves:

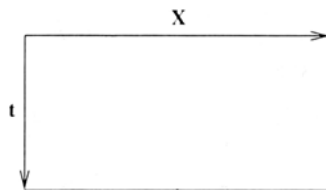
$$\frac{|\omega|}{|k_x|} > v \quad (15)$$

Equation (14) can be written in a recursive way, relating the solution at depth Z to the solution at depth $Z + \Delta Z$:

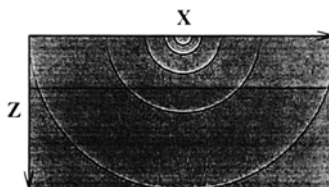
$$P(X, Z + \Delta Z, 0) = \sum_{k_x} \left\{ \sum_{\omega} P(k_x, Z, \omega) \exp(ik_z \Delta Z) \right\} \exp(ik_x X) \quad (16)$$

The expression in brackets is a summation over ω constrained by (15) for each increment ΔZ . We then must do a single inverse transform to recover the migrated section. Equation (16) is the basis for the "phase shift" method; it allows the inverse extrapolation of seismic data in layered media where the velocity field, a piecewise constant function of Z , varies from layer to layer.

To illustrate the phase shift method, we consider a synthetic seismic section, $P(X, 0, t) = \sum_i \delta(X - X_i) \delta(t - t_i)$, representing a signal equal to zero everywhere, except in a collection of points of the $(X, 0, t)$ plane. According to geometric seismics, the resulting migrated section in the



(a)



(b)

Fig. 4. Phase shift migration, semicircular mirrors x . (a) Seismic section, (b) resulting migrated section; $N_x = 256$, $N_z = N_t = 128$, $\Delta X = \Delta Z = 50$ m, $\Delta t = 50$ msec, $v = 1$ km/sec.

$(X, Z, 0)$ plane must represent points distributed along semicircular mirrors of radius vt_i and center $(X_i, 0, 0)$. Iterating Eq. (16), the computed solution shown in Fig. 4 is in full agreement with the expected result.

Figure 5 illustrates the direct and the inverse problem in a very simple example. A pointlike impulsive source, playing the role of one exploding reflector, is located in the $(X, Z, 0)$ plane (Fig. 5a). Such a reflector can be seen as a short-wavelength perturbation of the velocity field (see also Fig. 1). The seismic section $P(X, 0, t)$ is simulated by solving the scalar wave equation with constant velocity (Fig. 5b). The resulting migrated section $P(X, Z, 0)$ shows the accuracy of this approach (Fig. 5c). Remember that the artificial condition of periodic must be introduced along both X and t -axes.

Phase shift formulation of frequency domain migration is a good example of a problem leading to an elegant data parallel implementation,

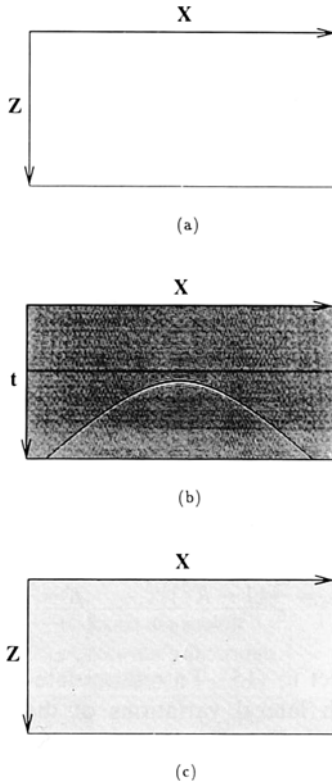


Fig. 5. Phase shift migration. (a) Pointlike reflector, (b) simulated seismic section, (c) resulting migrated section; $N_x = 256$, $N_z = N_t = 128$, $\Delta X = \Delta Z = 50$ m, $\Delta t = 50$ msec, $v = 1$ km/sec.

combining computation and communication among processors.⁽¹⁴⁾ To construct the migrated section using Eq. (16), a typical run starts with one 2D FFT, producing an array of complex numbers. For each complex array tagged by Z , a parallel operator masks all spurious frequencies and shift the phase of each entry. Second, “scan_with_add” operations over ω are concurrently performed, once for each k_x . These two steps are repeated for increasing values of Z . The run ends imaging the reflections, namely with the concurrent execution of 1D FFTs, one for each value of depth.

4.2. Migration in Inhomogeneous Media

We would like to migrate data using an arbitrary velocity model. It is clear from the construction of Eq. (16) that the phase shift formula is no longer valid for a velocity field $v = v(X, Z)$ with lateral variations. Nevertheless, assuming v periodic along the X axis and decomposing P and v^{-2} in Fourier series, the inverse problem may be solved. The difficulty with this approach is that it leads to the solution of a dense system of second-order ordinary differential equations for the Fourier coefficients $P(k_x, Z, \omega)$, for each value of Z . To avoid this cumbersome task, it is preferable to simplify the migration model a step further, keeping its computational complexity to a reasonable level.

The basic strategy adopted is the following.⁽¹⁵⁾ We start from the description of waves propagating downward through layered media, assuming momentarily that the velocity field is a piecewise constant function, varying from layer to layer. It is worthwhile noticing that under this condition, expression (13) is also a solution of

$$\frac{dP}{dZ}(k_x, Z, \omega) = ik_z P(k_x, Z, \omega) \quad (17)$$

which is the exact extrapolation equation in a layer $[Z; Z + \Delta Z]$ with velocity $v = v_z$. Remember that k_z takes only real values, we have

$$k_z = \frac{\omega}{v} (1 - K^2)^{1/2}, \quad K = \frac{vk_x}{\omega} \quad (18)$$

with k_x , ω , and v subject to (15). To reformulate the wave propagation in a layered medium with lateral variations of the velocity $v = v_z(X)$, the migration process governed by Eq. (17) must be somehow moved to the (X, ω) domain. For this purpose, we first approximate the square root $\mathcal{R} = (1 - K^2)^{1/2}$ by a truncated rational expansion in K . The simplest approximation is the Taylor series.⁽¹⁶⁾ A better alternative is to use faster

expansions of \mathcal{R} requiring fewer terms for the same accuracy.^(17,18) One popular form is the approximation of the square root by continued fractions,

$$\mathcal{R}_{n+1}^{cf} = 1 - \frac{K^2}{1 + \mathcal{R}_n^{cf}}, \quad \mathcal{R}_0^{cf} = 1 \tag{19}$$

However, a more accurate rational expansion is obtained by computing the square root with the Newton algorithm. This gives rise to the following recurrence relation:

$$\mathcal{R}_{n+1}^{nw} = \frac{1}{2} \left(\mathcal{R}_n^{nw} + \frac{1 - K^2}{\mathcal{R}_n^{nw}} \right), \quad \mathcal{R}_0^{nw} = 1 \tag{20}$$

To verify that both expansions converge to Eq. (18), just let $n \rightarrow \infty$ in Eqs. (19) and (20). Iterating both expressions twice, we obtain two approximations of the square root (Fig. 6):

$$\mathcal{R}_2^{cf} = 1 - \frac{K^2}{2 - \frac{1}{2}K^2} \tag{21}$$

$$\mathcal{R}_2^{nw} = 1 - \frac{K^2}{2} \frac{1 - \frac{1}{4}K^2}{1 - \frac{1}{2}K^2} \tag{22}$$

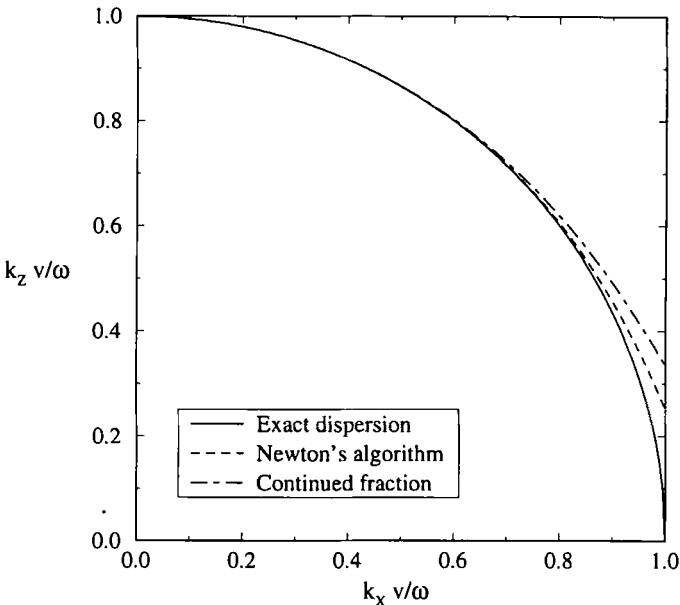


Fig. 6. Dispersion relations.

Substituting one of the two truncated expansions into Eq. (18), we obtain an approximation for the dispersion relation,

$$k_z = \frac{\omega}{v} + \mathcal{G}\left(\frac{v}{2\omega}, k_x\right) \quad (23)$$

From Eq. (21) it follows that

$$\mathcal{G}^{\text{cr}} = \frac{-(v/2\omega) k_x^2}{1 - (v/2\omega)^2 k_x^2} \quad (24)$$

while from Eq. (22)

$$\mathcal{G}^{\text{nw}} = -\left(\frac{v}{2\omega}\right) k_x^2 \left[\frac{1 - (v/2\omega)^2 k_x^2}{1 - 2(v/2\omega)^2 k_x^2} \right] \quad (25)$$

The consequent approximation of the downward extrapolation, Eq. (17), is written

$$\frac{dP}{dZ}(k_x, Z, \omega) = i \left[\frac{\omega}{v} + \mathcal{G}\left(\frac{v}{2\omega}, k_x\right) \right] P(k_x, Z, \omega) \quad (26)$$

Equation (26) can be solved using a fractional step method based on a factorization of the Crank–Nicholson scheme.⁽¹⁹⁾ The resulting numerical method is consistent with the system of equations

$$\frac{dP_0}{dZ}(k_x, Z, \omega) = \frac{i\omega}{v} P_0(k_x, Z, \omega), \quad P_0(k_x, Z, \omega) = P(k_x, Z, \omega) \quad (27)$$

$$\frac{dP}{dZ}(k_x, Z, \omega) = i\mathcal{G}P(k_x, Z, \omega), \quad P(k_x, Z, \omega) = P_0(k_x, Z + \Delta Z, \omega) \quad (28)$$

which is thus considered as the decomposed or split form of Eq. (26).

For any single step ΔZ , the solution of Eq. (27) is used as initial condition to Eq. (28). Note that Eq. (27) governs vertically-traveling waves with an infinite horizontal wavelength, $k_x = 0$, while Eq. (28) governs the horizontal correction.

Under the assumption of a homogeneous layer $[Z; Z + \Delta Z]$ with a constant velocity $v = v_z$, solving Eq. (27) is simply a multiplication of $P(k_x, Z, \omega)$ by a phase shift operator. This multiplication can be done in the (X, ω) domain:

$$P_1(X, Z, \omega) = P(X, Z, \omega) \exp\left(i \frac{\omega}{v} \Delta Z\right) \quad (29)$$

To express Eq. (28) in the (X, ω) domain, multiply by the denominator of \mathcal{G} and then take the inverse Fourier transform of the equation with respect to k_x . The equation can then be written as

$$\left[1 + \left(\frac{v}{2\omega} \right)^2 \frac{\partial^2}{\partial X^2} \right] \frac{\partial P^{cf}}{\partial Z} = \frac{iv}{2\omega} \frac{\partial^2 P^{cf}}{\partial X^2} \quad (30)$$

$$\left[1 + 2 \left(\frac{v}{2\omega} \right)^2 \frac{\partial^2}{\partial X^2} \right] \frac{\partial P^{nw}}{\partial Z} = \frac{iv}{2\omega} \frac{\partial^2}{\partial X^2} \left[1 + \left(\frac{v}{2\omega} \right)^2 \frac{\partial^2}{\partial X^2} \right] P^{nw} \quad (31)$$

with $P(X, Z, \omega) = P_1(X, Z, \omega)$, according to the choice of \mathcal{G} . Having expressed the problem in the (X, ω) domain, the control that we had in the (k_x, ω) domain on spurious waves is lost. However, a practical approach to masking them is to introduce an arbitrary cutoff of ω around zero. The migrated data at $Z + \Delta Z$ are obtained by

$$P(X, Z + \Delta Z, 0) = \sum_{\omega} P(X, Z + \Delta Z, \omega) \quad (32)$$

where the summation is carried out for all admissible ω . The implementation of Eq. (32) represents the imaging step of the migration process.

Equations (30) and (31) are two different approximations of the downward extrapolation in a layered medium. Although a further simplification has been introduced with respect to the initial inverse model, the advantage of the (X, ω) formulation is that the velocity field dependence is no longer restricted to the depth variable alone, but may also include lateral variations inside a single layer $[Z; Z + \Delta Z]$. The straightforward introduction of the velocity $v = v_z(X)$ in the extrapolating equations (29)–(31) can be questionable. Although it has no clear conceptual basis, it furnishes a migration model for inhomogeneous media which is surprisingly reliable on synthetic seismic data with reasonable changes of $v_z(X)$.

Equations (30) and (31) are solved numerically. Using the Crank–Nicholson scheme, P and $\partial P/\partial Z$ are evaluated at the midpoint of $[Z; Z + \Delta Z]$. Derivatives in X are approximated by central finite differences.⁽²⁰⁾ The inverse problem is thus transformed into a set of linear algebraic equations which must be solved for all admissible values of ω :

$$\begin{aligned} \mathbf{Q}(Z) &= \mathbf{P}(Z) \exp\left(i \frac{\omega}{v} \Delta Z\right) \\ \mathcal{A} \mathbf{P}(Z + \Delta Z) &= \mathcal{A}' \mathbf{Q}(Z), \quad \mathcal{A} = \mathcal{A}' \left(\frac{v}{2\omega} \right) \end{aligned} \quad (33)$$

\mathcal{A} is a nonsingular tri- or pentadiagonal complex matrix and \mathcal{A}^c its conjugate. Vector \mathbf{P} stands for the solution of Eq. (33), the finite-difference approximation of P . The spectral radius of the product of matrices ($\mathcal{A}^{-1}\mathcal{A}^c$) being equal to one, the advancing scheme (33) has the required property of stability to describe correctly the downward wave propagation.

To illustrate the approach, we consider the following synthetic seismic section: $P(X, 0, t) = \sum_i \delta(X - X_i) \delta(t - t_i)$ and $v = 1$. Equation (30) reflects the inaccuracy of the continued fraction approximation of the square root for $0.6 \leq K \leq 1$. This is shown in Fig. 7a: the solution produces a cardioid instead of the expected circle as in Fig. 6. This tendency is partially corrected with Eq. (31), even though a less accurate numerical scheme than that used for Eq. (30) was implemented for the example (Fig. 7b).

We illustrate the exploding reflector model with synthetic data. Figure 8a shows a distribution of reflectors acting as sources located in the $(X, Z, 0)$ plane. This source configuration is introduced in the scalar wave equation subject to the velocity field depicted in Fig. 8b. The seismic section, solution of Eq. (9) in the $(X, 0, t)$ plane, is shown in Fig. 8c. With the inverse problem we attempt to reconstruct Fig. 8a solving Eq. (30) and imaging the reflectors using Eq. (32). Figure 8d illustrates the quality of the migration process.

The finite-difference formulation of the inverse extrapolation in the (X, ω) domain is another good example of a problem leading to an elegant

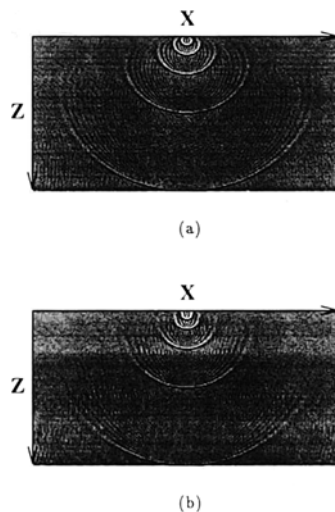


Fig. 7. Approximated semicircular mirrors, k_z is expanded by (a) continued fraction, (b) Newton's algorithm. Compare with Fig. 4.

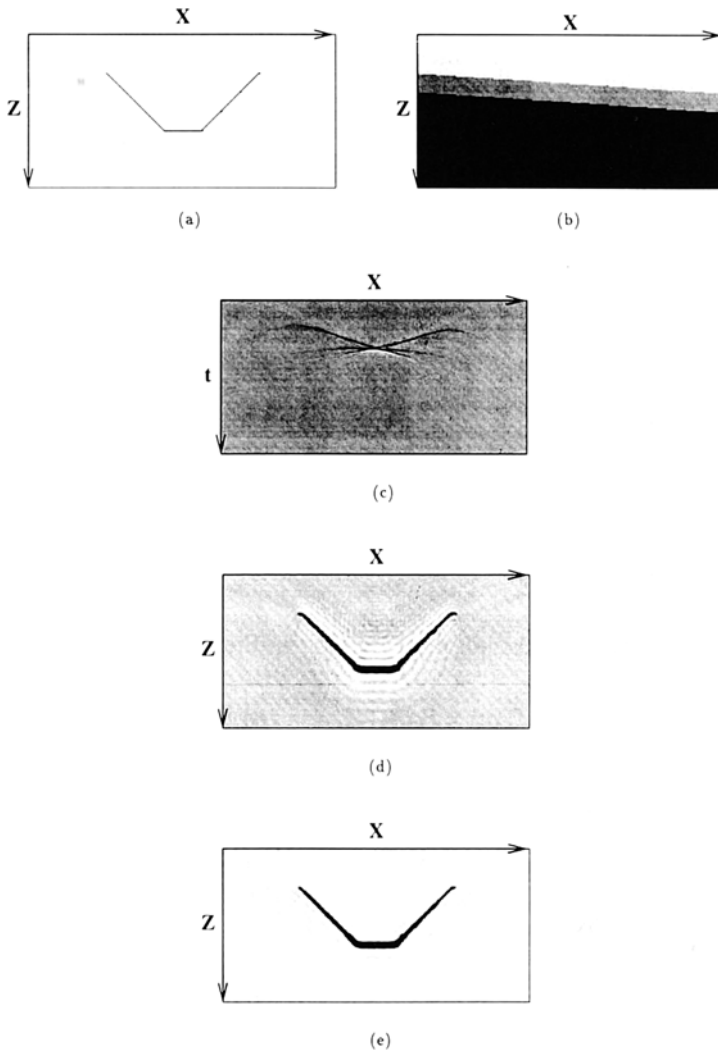


Fig. 8. Migration of synthetic data in inhomogeneous medium. (a) Reflector; (b) inhomogeneous velocity field, v varies from 1 to 4 km/sec; (c) simulated seismic section; (d) finite difference, Eq. (30): migrated section; (e) phase shift plus interpolation: migrated section; $N_x = 256$, $N_z = N_t = 128$, $\Delta X = \Delta Z = 50$ m, $\Delta t = 50$ msec.

data-parallel implementation. A typical run starts with the concurrent execution of 1D FFTs, one for each X , producing an array of complex numbers. For each horizontal layer, a parallel operator masks all spurious frequencies and shifts the phase of each entry of the complex array, preparing data for the solution of Eq. (30). The resulting linear systems, parametrized by ω , are concurrently solved. Finally, the imaging of reflectors is performed, running concurrent “scan_with_add” operations over ω for each value of X , according to Eq. (32).

4.3. Migration by Phase Shift plus Interpolation

The purpose now is to construct a pure spectral method for the extrapolation of seismic data in an inhomogeneous medium. The point is to keep the computation in the (k_x, ω) domain, avoid the less accurate finite-difference solution of partial differential equations in the (X, ω) domain.

We start from Eq. (26), decomposed into Eqs. (27) and (28), under the assumption of a homogeneous layer $[Z; Z + \Delta Z]$ with a constant velocity $v = v_z$. The solution of Eq. (27) in the (X, ω) domain takes the form

$$P_0(X, Z, \omega) = P(X, Z, \omega) \exp\left(i \frac{\omega}{v} \Delta Z\right) \quad (34)$$

Since $\mathcal{G} = k_z - \omega/v$, the solution of Eq. (28) in the (k_x, ω) domain becomes

$$P(k_x, Z + \Delta Z, \omega) = P_0(k_x, Z, \omega) \exp\left[i \left(k_z - \frac{\omega}{v}\right) \Delta Z\right] \quad (35)$$

The extrapolators (34) and (35) represent the split form of the phase shift operator.

Equation (34) is formulated in the (X, ω) domain and can be formally computed with $v = v_z(X)$. In contrast, Eq. (35) is not formally valid when the velocity varies laterally; however, supposing the equation piecewise-valid, it is evaluated at different velocities to construct the solution in the (X, ω) domain.⁽²⁰⁾

To explain, let us consider a sampling of $v = v_z(X)$, including the smallest and the largest velocity values: $v_{\min} = v_0 < v_1 < v_2 < \dots < v_{M+1} = v_{\max}$. Introducing each one of them into Eq. (35), we can extrapolate the pressure field $P_0(k_x, Z, \omega)$, velocity after velocity, and represent each result in the (X, ω) domain:

$$P^{(n)}(X, Z + \Delta Z, \omega) = \sum_{k_x} P_0(k_x, Z, \omega) \exp\left[i \left(k_z^{(n)} - \frac{\omega}{v_n}\right) \Delta Z + k_x\right] \quad (36)$$

with $n = 0, 1, 2, \dots, M + 1$. To avoid the propagation of spurious waves, k_x , ω , and v_n are subject to condition (15).

The transformed fields $P^{(n)}(X, Z + \Delta Z, \omega)$ serve as reference data from which the final result will be obtained by interpolation:

$$P(X, Z + \Delta Z, \omega) = \sum_{n=0}^{M+1} P^{(n)}(X, Z + \Delta Z, \omega) \phi^n(X) \quad (37)$$

ϕ^n is the shape function whose support is defined by the reference velocities v_{n-1} and v_{n+1} bounding $v_z(X)$. For instance, in the case of linear interpolation,

$$\phi^n(X) = \begin{cases} \frac{v_z(X) - v_{n-1}}{v_n - v_{n-1}} & \text{where } v_{n-1} \leq v_z(X) \leq v_n \\ \frac{v_{n+1} - v_z(X)}{v_{n+1} - v_n} & \text{where } v_n \leq v_z(X) \leq v_{n+1} \\ 0 & \text{otherwise} \end{cases} \quad (38)$$

Substituting Eq. (38) into (37), the interpolated solution becomes

$$P(X, Z + \Delta Z, \omega) = P^{(n)}(X, Z + \Delta Z, \omega) \frac{v_{n+1} - v_z(X)}{v_{n+1} - v_n} + P^{(n+1)}(X, Z + \Delta Z, \omega) \frac{v_z(X) - v_n}{v_{n+1} - v_n} \quad (39)$$

for all X such that $v_n \leq v_z(X) \leq v_{n+1}$.

Finally, the imaging of the reflectors at $Z + \Delta Z$ is obtained by

$$P(X, Z + \Delta Z, 0) = \sum_{\omega} P(X, Z + \Delta Z, \omega) \quad (40)$$

The phase shift plus interpolation is a practical alternative to the finite-difference migration in the (X, ω) domain with the obvious advantage that each reference velocity gives rise to an analytic solution, Eq. (36). This is the essence of the phase shift plus interpolation. All reference solutions can be concurrently computed using the phase shift algorithm. Equation (39) can be evaluated using the data parallel "where" construct.⁽¹⁴⁾

Here again, the introduction of laterally-variable velocities and the use of interpolating reference solutions do not have a well-established mathematical basis. Computer experiments show that this approach is in fact

more reliable than finite differences in the (X, ω) domain.⁽²⁰⁾ Neither model will perform well when velocity contrast in X is too strong. However, the obvious advantage of finite differences is that the resulting algorithm is faster because the use of 2D or 3D FFTs is not necessary.

Reference velocities are chosen, for instance, to form a geometric progression $(v_{n+1}/v_n) = R$, $n = 0, 1, 2, \dots, M$; the number M is the smallest integer for which we have $(v_{\text{Max}}/v_{\text{min}}) \geq R^{M+1}$.

We illustrate the phase shift plus interpolation with the synthetic seismic section and the velocity field of Figs. 8c and 8d. In this example, the number of reference velocities is 5 and $R = 1.5$. The comparison between Figs. 8e and 8a shows the quality of the inversion process in this case.

5. CONCLUSION

This article is concerned with 2D migration after common midpoint stacking. We have described the migration of zero-offset seismic data using the scalar wave equation. First, assuming periodicity in X and t of the pressure field, we present a downward extrapolation equation in the (k_x, ω) domain, exact for layered media. Then we consider media with inhomogeneities in X as well as Z and reformulate the model to describe migration in the (X, ω) domain. Alternatively, we show how the original downward extrapolation equation in (k_x, ω) can be used with various reference velocities to give an interpolation in (X, ω) of the pressure field for inhomogeneous media.

Data parallelism (on a CM-200 with 8k one-bit processors under the slicewise execution model) has allowed us to take advantage of the natural concurrency in seismic migration models. This is important for field applications in oil and gas exploration, in which extensive computation on huge data sets is necessary for the 3D reconstruction of acoustic subsurface images. With the increase in computing power, pre-stack inversion is becoming feasible.

We note that the most computationally demanding problems in natural science, including tomography, image processing, satellite imaging, etc., can benefit from reformulations that enhance intrinsic concurrence.

ACKNOWLEDGMENTS

We are very much indebted to Pietro Rossi and Leesa Brieger for many stimulating discussions. This work was supported by the Regional Authority of Sardinia.

REFERENCES

1. K. C. Jain and R. J. P. de Figueiredo, eds., *Concepts and Techniques in Oil and Gas Exploration* (SEG, 1982).
2. J. A. Scales, *An Introductory Course on Seismic Migration* (Colorado School of Mines, 1993).
3. A. Tarantola, Inversion of seismic reflection data in the acoustic approximation, *Geophysics* **49**:1259 (1984).
4. A. Tarantola, *Inverse Problem Theory, Methods for Data Fitting and Model Parameter Estimation* (Elsevier, 1987).
5. P. Kolb, F. Collino, and P. Lailly, Pre-stack inversion of a 1D medium, *Proc. IEEE* **74**:498 (1986).
6. A. Pica, J. P. Diet, and A. Tarantola, Nonlinear inversion of seismic reflection data in a laterally invariant medium, *Geophysics* **55**:284 (1990).
7. A. D. McAulay, Plane-layer prestack inversion in the presence of surface reverberation, *Geophysics* **51**:1789 (1986).
8. B. Biondi, Velocity estimation by beams stack, *Geophysics* **57**:1034 (1992).
9. S. V. Goldin, *Seismic Traveltime Inversion* (Society of Exploration Geophysicists, 1986).
10. R. H. Stolt, Migration by Fourier transform, *Geophysics* **43**:23 (1978).
11. L. L. Liu, 3-D Prestack Kirchhoff migration: Parallel computation on workstations, in *Technical Program: Expanded Abstracts* (SEG 63rd Annual Meeting and International Exhibition, Washington D.C., 1993).
12. F. L. Rocca and L. B. Salvador, *Migration in Seismic Processing* (Quaderni di Geofisica Q-003, DES/AGIP, 1985).
13. N. S. Neidell and M. Turnhan Taner, Semblance and other coherency measures for multi-channel data, *Geophysics* **36**:482 (1971).
14. *Connection Machine CM-200 Series Technical Summary* (Thinking Machines Corporation, Cambridge, Massachusetts, 1991).
15. E. A. Robinson, Migration of seismic data as W.K.B. approximation, *Geoexploration* **20**:7 (1982).
16. J. Gazdag, Wave equation migration with the accurate space derivative method, *Geophys. Prospecting* **28**:60 (1980).
17. P. G. Kelamis, On the theory of Chebyshev polynomial in wave-equation migration, *Geophys. J.* **94**:421 (1988).
18. D. Hale, Stable explicit depth extrapolation of seismic wavefields, *Geophys. Prospecting* **56**:1770 (1991).
19. Zh. Li, Compensating finite-difference errors in 3-D migration and modeling, *Geophysics* **56**:1650 (1991).
20. J. Gazdag and P. Sguazzero, Migration of seismic data, *Geophysics* **49**:124 (1984).